2D NOESY of palladium .pi.-allyl complexes. Reporter ligands, complex dynamics, and the x-ray structure of [Pd(.eta.3-C4H7)(bpy)](CF3SO3) (bpy = bipyridine)

Alberto. Albinati, Roland W. Kunz, Christian J. Ammann, and Paul S. Pregosin

Organometallics, **1991**, 10 (6), 1800-1806• DOI: 10.1021/om00052a028 • Publication Date (Web): 01 May 2002

2D NOESY of Palladium π-Allyl Complexes. Reporter Ligands, Complex Dynamics, and the X-ray Structure of $[Pd(\eta^3\text{-}C_4H_7)(bpy)](CF_3SO_3)$ (bpy = Bipyridine)

Alberto Albinati

Istituto di Chimica Farmaceutica, Università di Milano, I-20131 Milano, Italy

Roland W. Kunz

Organisch-chemisches Institut, Universität Zürich, CH-8057 Zürich, Switzerland

Christian J. Ammann and Paul S. Pregosin*

Laboratorium für Anorganische Chemie ETH-Z, CH-8092 Zürich, Switzerland

Received August 28, 1990

Cationic Complexes of the type $Pd(\eta^3\text{-}C_4H_7)(N\frown N)^+$ ($C_4H_7 = CH_2C(CH_3)CH_2$; N⌒N = a variety of nitrogen chelates) have been studied by ^1H 2D NOESY. The strengths and weaknesses of the concept of reporter ligands are discussed, and the allyl C–H rehybridization found in earlier studies is confirmed for the η^3-(2-methylallyl) ligand. Aspects of the dynamics of these cations are discussed. Calculations for $Pd(\eta^3\text{-}C_4H_7)(bpy)^+$ (bpy = bipyridine), based partially on the solution NOE results, afford a solution structure, which is in good agreement with the structure (CF_3SO_3 anion) determined by X-ray diffraction methods. The complex crystallized in the space group $P2_1/c$ with a = 7.185 (1) Å, b = 16.762 (1) Å, c = 14.811 (1) Å, β = 95.593 (9)°, V = 1775.3 Å^3, and Z = 4. Selected bond distances: Pd–N(1) = 2.089 (2) Å, Pd–N(2) = 2.085 (3) Å, Pd–C(7) = 2.095 (4) Å, Pd–C(8) = 2.123 (4) Å, and Pd–C(9) = 2.112 (4) Å. From both the solution and solid-state structures we find distances from the bipyridine ortho proton, H(6), to the allyl syn and anti protons to be ca. 2.8–2.9 and 3.1–3.5 Å, respectively.

Introduction

Although two-dimensional NMR spectroscopy is almost routine in some respects, the structural side, i.e., NOESY, has been somewhat neglected in the organometallic community. NOESY is a particularly useful methodology, since the same phase-sensitive spectrum can deliver both exchange and Overhauser data when protons are considered.[1,2] In recent work we have developed the idea of reporter ligands,[3] whose "job" it is to detect structural features—both gross and subtle—by using suitably placed proton spins that "see" across a metal via an Overhauser effect. This approach has led to aspects of the 3D structures for π-allyl complexes of (a) optically active nitrogen chelating ligands[4] (b) 2,2′-bis(diphenylphosphino)-naphthalene (BINAP),[5] and (c) relatively simple aromatic nitrogen ligands, e.g., $Pd(\eta^3\text{-}C_6H_{10})(biquinoline)^+$, for which we have reported the molecular structure.[3] This latter complex and a number of related complexes containing phenanthroline and bipyridine ligands were useful in demonstrating that the rehybridization of the terminal allyl C–H bonds is not the same for both the syn and anti protons. Indeed, the anti hydrogen bends ca. 30° away from the palladium, thereby distancing itself from the nitrogen chelate reporter proton. This distortion in allyl complexes is rather general and has been observed in the solid state both with X-rays[6,7] and neutrons[8] and has been rationalized theoretically.[9]

Chart I

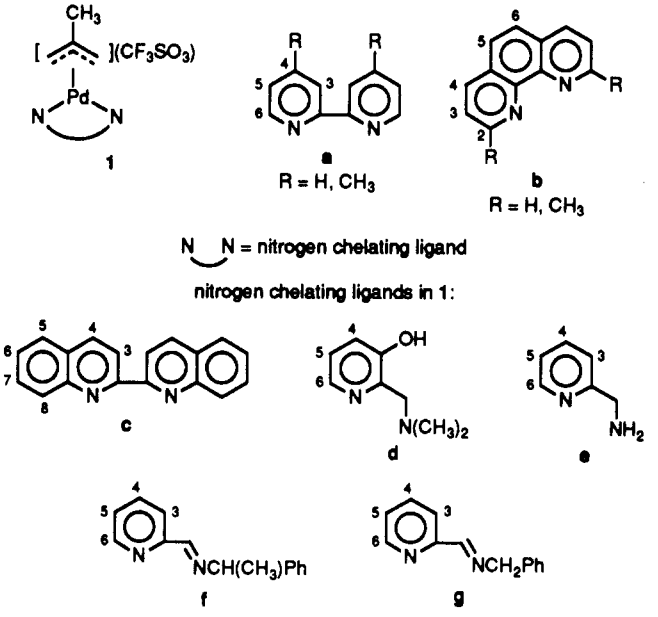

We report here an extension of our basic idea in that we (1) expand on the type of reporter chelate, (2) demonstrate the generality of the allyl distortion, (3) introduce a chiral center on one side of a reporter in connection with palladium π-allyl dynamics, (4) supplement our "solution structure" with modeling studies, and (5) confirm the validity of our solution structure with the X-ray structure of $[Pd(\eta^3\text{-}C_4H_7)(bpy)](CF_3SO_3)$ (bpy = bipyridine).

Results and Discussion

NMR Spectroscopy. Applications of ^1H NMR spectroscopy for palladium π-allyl complexes are widespread,[10–14] and we have little new to add with respect to

(1) Pregosin, P. S. *Pure Appl. Chem.* **1989**, *61*, 1771.
(2) Musco, A.; Pontellini, R.; Grossi, M.; Sironi, A.; Meille, S. V.; Rüegger, H.; Ammann, C.; Pregosin, P. S. *Organometallics* **1988**, *7*, 2130.
(3) Albinati, A.; Ammann, C.; Pregosin, P. S., Rüegger, H. *Organometallics* **1990**, *9*, 1826.
(4) Togni, A.; Rihs, G.; Pregosin, P. S.; Ammann, C. *Helv. Chim. Acta* **1990**, *73*, 723.
(5) Rüegger, H.; Kunz, R. W.; Ammann, C.; Pregosin, P. S. Submitted for publication in *Magn. Reson. Chem.*
(6) Gozum, J. E.; Pollina, D. M.; Jensen, J. A.; Girolami, G. S. *J. Am. Chem. Soc.* **1988**, *110*, 2688.
(7) Faller, J. W.; Blankenship, C.; Whitmore, B. *Inorg. Chem.* **1985**, *24*, 4483.
(8) Goddard, R.; Krüger, C.; Mark, F.; Stansfield, R.; Zhang, X. *Organometallics* **1985**, *4*, 285.
(9) Clark, T.; Rohde, C.; Schleyer, P. R. *Organometallics* **1983**, *2*, 1344.
(10) Shaw, B. L.; Shaw, G. *J. Chem. Soc. A* **1971**, 3533.
(11) Tsukiyama, K.; Takahashi, Y.; Sakai, S.; Ishii, Y. *J. Chem. Soc. A* **1971**, 3112.

0276-7333/91/2310-1800$02.50/0

Table I. Selected ^1H and ^{13}C Data (δ) for Complexes 1 and 2 with Ligands a–g

	a[a]		b[a]					f[b,j]		
	H^c	CH_3[d]	H^e	CH_3[f]	c[a,g]	d[b,h]	e[b,i]	major	minor	g[b,k]
					^1H					
syn	4.29	4.24	4.50	4.78	4.50	3.72[h]	3.94[i]	3.99[j]	3.99	3.97[k]
						3.70	3.76	3.37	3.07	3.27
anti	3.52	3.47	3.64	3.70	3.90	3.11	2.87	3.13[j]	3.17	3.14[k]
						3.11	3.09[i]	2.26	2.64	2.58
CH_3	2.30	2.29	2.36	2.22	2.20	2.19	2.13	1.88	1.88	1.84
					^{13}C					
allyl $^{13}CH_2$	61.2[c]	60.8[d]	61.3[e]	62.6[f]	64.1	59.2	56.4	59.2	59.6	59.8
						61.0	61.2	63.0	63.0	62.5

[Pt(η³-C_4H_7)(g)](CF_3SO_3)[l]				2[p]				
	^1H		^{13}C		2a (major)		2b (minor)	
					^1H	^{13}C	^1H	^{13}C
syn	3.79[m] (25)	CH	46.7[m,n] (228)	allyl CH_2	3.58 (syn)	60.1	3.70 (syn)	59.0
	3.28 (25)				3.25 (anti)		3.36 (anti)	
anti	2.78[m] (70)	CH	43.8 (241)	allyl CH	3.95	67.1	3.95	67.8
	2.26 (74)		123.8[o] (83)					
CH_3	1.87 (82)	CH_3	23.8 (47)	NCH_3	2.80, 2.90	53.1, 51.3	2.80, 2.57	50.9, 50.1
NCH_2	5.44 (40)	CH_2	68.3 (70)	NCH_2	4.10 (AB spin syst)	67.9	4.03, 4.34	68.7

[a] Acetone-d_6, room temperature. [b] $CDCl_3$, room temperature. [c] H(6), 9.07; C(6), 154.0. [d] H(6), 8.90; CH_3, 2.62; C(6), 153.4; CH_3, 21.5. [e] H(2), 9.45; C(2), 154.4. [f] CH_3, 3.14; C(2), 153.4; CH_3, 21.5. [g] H(8), 8.57; C(8), 129.3; C(2), 156.3. [h] H(6), 8.02; NCH_2, 4.04, 4.17; NCH_3, 2.85, 2.94; δ 3.72 opposite to H(6); C(2), 153.3; C(6), 143.8; NCH_2, 64.1; NCH_3, 52.0, 53.1. [i] H(6), 8.56; NCH_2, 4.47; NH_2, 4.47 (overlaps CH_2); 53.94, 3.09 opposite to H(6); C(2), 162.8; C(6), 152.4; NCH_2, 50.2. [j] Major: H(6), 8.78; C*H*=N, 9.19; CH, 5.19, CH_3, 1.74; C(2), 153.6; C(6), 154.1, *C*H=N, 167.8; *C*H, 68.4; CH_3, 20.4. Minor: H(6), 8.78; C*H*=N, 9.14; CH, 5.19; CH_3, 1.70; C(2), 153.7; C(6), 154.1; CH=N, 167.3; *C*H, 68.6; CH_3, 20.6. [k] H(6), 8.76; C*H*=N, 9.11; NCH_2, 5.13; 3.97, 3.14 opposite to H(6); C(2), 153.9; C(6), 154.3; *C*H=N, 169.9; NCH_2, 66.8. [l] $CDCl_3$, room temperature; values in parentheses are *J*(Pt,X). [m] Opposite to H(6). [n] Confirmed via ^{13}C, ^1H proton correlation. [o] Central allyl carbonyl. [p] ^{13}C signals are as follows. **2a**: pyridine C's 2–6, 159.3, 124.1, 140.5, 125.5, 149.6; central allyl, 144.2; aliphatic C's D–I, K, 33.8, 39.5, 29.5, 46.4, 37.9, 25.9, 21.9. **2b**: pyridine 158.2, 124.4, 140.3, 125.3, 153.4; aliphatic central allyl, 144.9; aliphatic C's D–I, K, 34.3, 39.5, 29.5, 46.4, 37.9, 25.9, 21.9. ^1H signals are as follows. **2a**: CH^h_3, 0.98; CH^i_3, 1.30. **2b**: CH^h_3, 0.98; CH^i_3, 1.30.

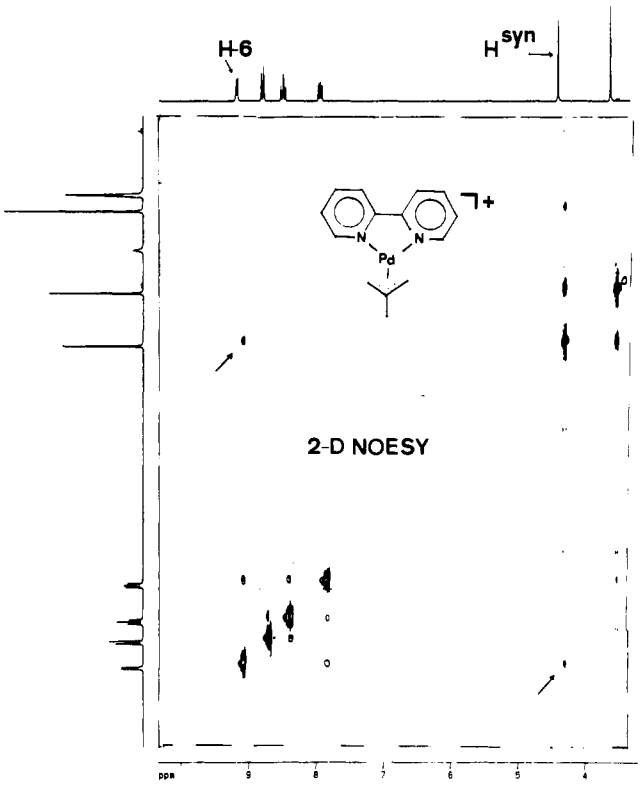

Figure 1. ^1H 2D NOESY spectrum of Pd(η³-C_4H_7)(bpy)⁺ (**1a**, R = H). Note that there are cross peaks connecting H(6) and the syn allyl proton but no cross peak from H(6) to the anti allyl proton (acetone-d_6, 250 MHz).

chemical shifts and coupling constants. A summation of our data is shown in Table I. As we have studied bi-

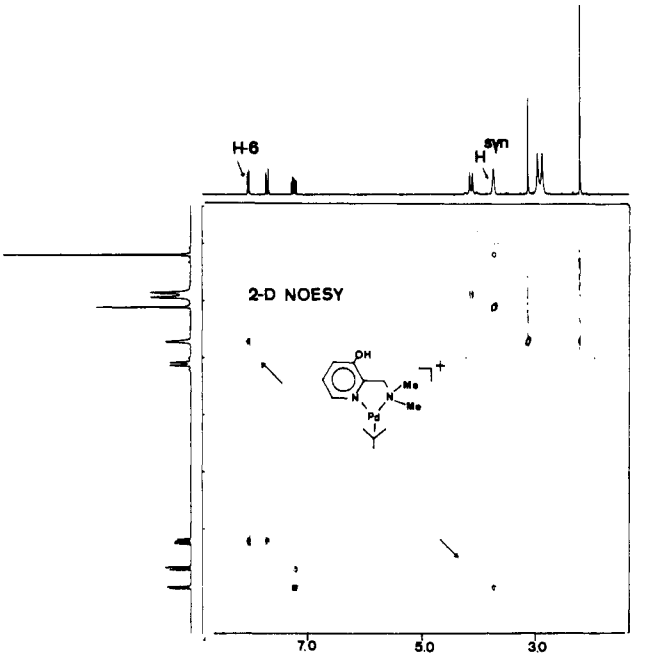

Figure 2. Section of the ^1H 2D NOESY spectrum of Pd(η³-C_4H_7)(**d**)⁺. Note that the H(6) proton has a cross peak with one of the two syn protons (both overlap at this temperature) but no cross peak to the two resolved, but broad, anti allyl protons at ca. 3.0 ppm (acetone-d_6, 250 MHz, ambient temperature).

pyridine, phenantholine, and biquinoline with C_6 and C_{10} allyl ligands previously, we start our discussion with the ^1H 2D NOESY for Pd(η³-C_4H_7)(bpy)⁺ (**1a**, R = H) (see Chart I), which is a methylallyl analogue of our previous

(12) Mabbott, D. J.; Mann, B. E.; Maitlis, P. M. *J. Chem. Soc., Dalton Trans.* **1977**, 294.

(13) Crociani, B.; Di Bianca, F.; Giovenco, A.; Boschi, T. *Inorg. Chim. Acta* **1987**, *127*, 169.

(14) Hayashi, A.; Matsumoto, K.; Nakamura, Y.; Isoba, K. *J. Chem. Soc., Dalton Trans.* **1989**, 1519.

complexes. The ^1H 2D NOESY spectrum of cation **1a** is shown in Figure 1 and reveals a selective NOE (cross peaks noted with arrows) from the ortho protons of the pyridine rings to the syn protons of the π-allyl. This selectivity, which we also observe in the corresponding 2D spectrum of the phenanthroline analogue, **1b**, R = H, is consistent with bending of the anti proton ca. 30° out of the allyl plane and away from the metal.[3] The biquinoline complex, **1c**, R = H, shows strong NOE's to *both* the syn and anti protons from H(8). Consequently, this is a nonselective but nevertheless useful "reporter". For completion,[15] we note the strong NOE between the geminal allyl protons as well as an NOE between the CH_3 and the syn proton.

Having established this groundwork for aromatic nitrogen ligands, it is useful to extend the idea of NOE selectivity (positive or negative) to chelate nitrogen ligands that contain different nitrogen donors, e.g., **d–f**. Interligand NOE's in such complexes would allow us to readily assign spectra and, more importantly, help us to define the limits at which we might expect useful Overhauser enhancements. Figure 2 shows a section of the proton 2D NOE spectra for the 2-(dimethylamino)-3-hydroxypyridine cation $Pd(\eta^3\text{-}C_4H_7)(\mathbf{d})^+$. At room temperature (Figure 2) the 2D NOESY reveals the expected selective NOE from H(6), ortho to the pyridine nitrogen, to the syn allyl proton in the cis position (note that at this temperature the two syn protons overlap and the N–CH_3's are broad). As usual we do not observe an H(6), H^{anti} NOE. Interestingly, we do not find evidence for a significant N–CH_3, allyl proton NOE. It would seem that the approximate sp^3 hybridization at dimethylamino nitrogen results in CH_3 groups which are displaced away from the metal and the allyl and, consequently, make poor reporters in our context.

For $Pd(\eta^3\text{-}C_4H_7)(\mathbf{e})^+$, in which we have protons bound directly on the sp^3 nitrogen, we observe the usual H(6), H^{syn} NOE but no sign of N–H to allyl proton NOE. It is possible, but not necessary,[16] that these N–H protons exchange. We cannot be certain, since there is considerable overlap between the NH_2 and NCH_2 resonances; however, the extensive fine structure on this complicated multiplet suggests that the amine protons do not exchange but simply are poorly placed to develop considerable NOE with the allyl ligand. In a similar fashion $Pd(\eta^3\text{-}C_4H_7)(\mathbf{f})^+$ reveals H(6), H^{syn} NOE but no NOE stemming from the aliphatic or aromatic resonances of the $CH(CH_3)Ph$ moiety. In short, ligands **d–f** have one side of the nitrogen chelate that is "invisible" to the allyl.

In summary, it is possible to choose chelating nitrogen ligands with protons so positioned that they (a) detect selective distortions, (b) "see" both the syn and anti protons, or (c) see neither of these protons.

As might be expected from some of the line widths in Figure 2, our complexes $Pd(\eta^3\text{-}C_4H_7)(N\frown N)^+$ are dynamic on the NMR time scale at room temperature. Two-dimensional ^1H NMR spectroscopy, when measured in the phase-sensitive mode,[17] allows the detection of both NOE and exchange effects simultaneously. There is much known[18] with respect to dynamics in Pd(II) π-allyl complexes, so that we choose to restrict our comments on this

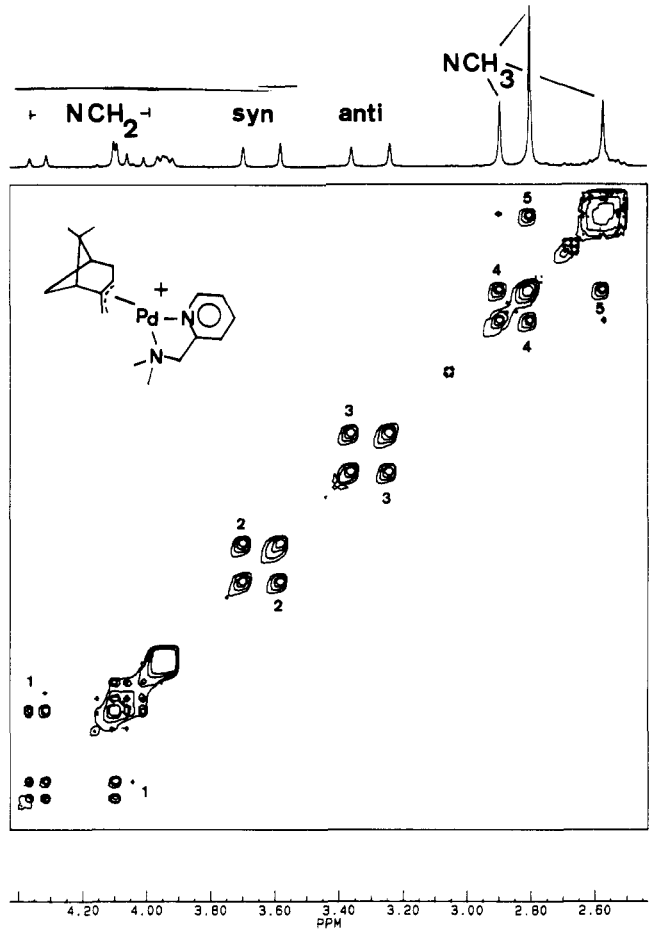

Figure 3. Section of the ^1H 2D exchange spectrum for $Pd(\eta^3\text{-}C_{10}H_{15})(2\text{-}Me_2NCH_2C_5H_4N)^+$ (**2**). The cross peaks 2 and 3 show syn–syn and anti–anti exchange, but the absence of cross peaks between the syn and anti protons elimintes η^3–η^1 as a pathway. In the NCH_2 region, there are two AB quartets, one of which at ca. 4.1 ppm is tightly coupled. In the N–CH_3 region two CH_3's from different isomers overlap. The broad signals at ca. 4.0 stem from the allyl C–H. ($CDCl_3$, 300 MHz).

subject to the complexes $Pd(\eta^3\text{-}C_4H_7)(\mathbf{f})^+$ and the somewhat contrived $Pd(\eta^3\text{-}C_{10}H_{15})(2\text{-}Me_2NCH_2C_5H_4N)^+$ (**2**).

Since ligand **f** contains an optically active center and as the Pd is a second center of chirality, we observe two diastereomers[19] in the NMR spectrum of $Pd(\eta^3\text{-}C_4H_7)(\mathbf{f})^+$. We note that the ^1H spectra are identical starting from either the pure R, pure S, or racemic mixture (relative to the amine carbon), in keeping with this second chirality center. The positive (exchange) cross peaks in the 2D NOESY spectrum for this ca 45:55 mixture of diastereomers reveal exchange between analogous protons of the two diastereomers but no exchange between protons within one diastereomer. There are no cross peaks between the syn and anti protons (in the phase-sensitive NOESY) thereby excluding an η^3–η^1 type isomerization. Apart from the η^3-η^1 possibility, there are a number of mechanisms for the isomerization,[20] including π-allyl rotation (with or without prior Pd–N bond breaking) and intermolecular reaction via 5-coordinate complexes.

Conventional wisdom suggests that the rotation of a π-allyl complex, with consequent reorganization of the various types of bonding, is "impossible for palladium".[20] There are, however, cases where π-allyl complexes with

(15) We have measured 2D NOESY spectra for ligands **a** and **b** (R = CH_3), and although the corresponding NOE's are present, these ligands offer no advantage relative to their R = H analogues.

(16) Pt(II)-coordinated oxazolidines show ^3J(H–N–C–H) values; see: Albinati, A.; Arz, C.; Pregosin, P. S. *J. Organomet. Chem.* **1989**, *371*, C18.

(17) Phase-sensitive detection affords exchange signals with the same phase as the diagonal and NOE cross peaks with phase opposite to the diagonal. The operator selects the "positive" or "negative" signals after phase correction.

(18) Vrieze, K.; Volger, H. C.; van Leeuwen, P. W. N. M. *Inorg. Chim. Acta Rev.* **1969**, 109.

(19) Faller, J. W.; Thomsen, M. E. *J. Am. Chem. Soc.* **1969**, *91*, 6871.

(20) Vrieze, K. In *Dynamic Nuclear Magnetic Resonance Spectroscopy*; Jackman, L. M., Cotton, F. A., Eds.; Academic Press: New York, 1975.

monodentate amines isomerize via dissociation of the nitrogen ligand.[21a] Ligand dissociation followed by isomerization is also known for π-allyl complexes with $SnCl_3$[21b] and CO.[30a] Moreover, one could imagine an "allyl-flip" mechanism, but this could result in syn–anti exchange, so that we choose to exclude this situation. In view of the possibility that our exchange might occur via dissociation of one of the two chelate nitrogen bonds, we have pursued the dynamics and consider now complex **2**; see Figure 3.

For **2**, where we again have two possible isomers, we find exchange between analogous protons of the two isomers, e.g., the two H(6) resonances in **2a** and **2b**, the two anti

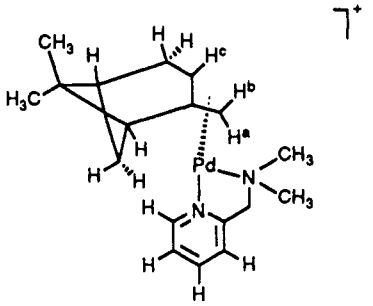

2a

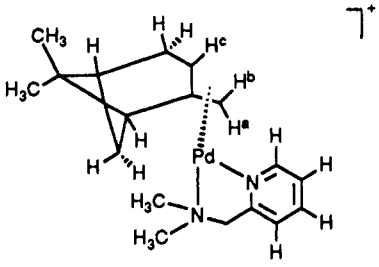

2b

protons H^b, but more importantly, the N–CH_3 (and N–CH_2) protons exchange from one isomer to another but *not* intramolecularly![30b] Once again there is no η^3–η^1 isomerization. If we assume that allyl does not rotate, then we may accommodate all of these observations for both complexes with a mechanism involving (a) dissociation of one of the Pd–N bonds, followed by (b) rotation around the remaining Pd–N bond, (c) isomerization of the T-shaped intermediate,[22] and (d) remaking of the Pd–N bond. Steps b and c may be inverted. As we find no intramolecular exchange between the two N–CH_3 groups,[30b] i.e., only N–CH_3 exchange between isomers, dissociation of an N–$(CH_3)_2$– fragment and subsequent steps must proceed without inversion at nitrogen—a process recognized to have a relatively low energy barrier—since such an inversion coupled with rotation about the $(CH_3)_2$N–C bond would exchange the two N–CH_3 groups. Naturally, all of our observations for **2** would fit an exchange mechanism arising from initial dissociation of the pyridine nitrogen. In this context Li et al.[23] have reported equilibrium constants for the reaction shown in eq 1 whereby K values for L =

$$[Pd(\eta^3\text{-}C_4H_7)Cl]_2 + 2L \rightarrow 2Pd(\eta^3\text{-}C_4H_7)ClL \quad (1)$$

pyridine, piperidine, and quinuclidine are 2.3×10^3, 1.4×10^5, and "large", respectively, so that pyridine nitrogen is not necessarily a much better donor than aliphatic nitrogen. One could argue that we should consider isomerization pathways which involve five-coordinate complexes. Our experience is that adding a chelating ligand does not influence the isomerization[24]—indeed, we find no exchange of the free and bound ligands—and this observation has been reported earlier[13] in a related complex. Further, we have measured a few activation energies (see Experimental Section) for the isomerization and for the same process with and without additional H_2O. The exchange rate is the same within the experimental error. Nevertheless, we cannot rigorously exclude exchange via a five-coordinate, perhaps even weak coordination of triflate,[30c] so that despite our efforts we do not know how this process of isomerization proceeds. Our four-step suggestion seems rather cumbersome but is consistent with our results, but so is an allyl rotation (for which there is some precedence)[25] as well as Cl^--catalyzed isomerization via a five-coordinate species ($CDCl_3$ decomposition). We consider this matter unresolved, but interesting, in that it touches the question of dissociation of one arm of a chelate, a subject of potential general interest.

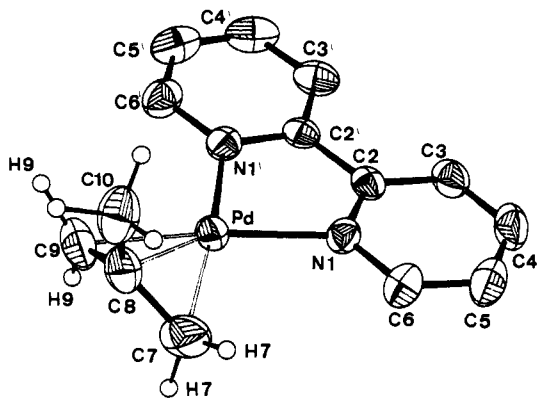

Figure 4. ORTEP view of the cation of $[Pd(\eta^3\text{-}C_4H_7)(bpy)](CF_3SO_3)$.

For purposes of general comparison we have also prepared one platinum complex, $[Pt(\eta^3\text{-}C_4H_7)(\mathbf{g})](CF_3SO_3)$, and note the following: (i) the NOE behavior (H(6) to syn proton, nonobservable to CH_2 from the allyl) is identical with that of the palladium analogue for the allyl protons; (ii) the ^2J(Pt,H) values for the allyl protons do not suggest significant differences in the donor capacity of the two nitrogen ligands; (iii) there is no exchange at room temperature, whereas the $[Pd(\eta^3\text{-}C_4H_7)(\mathbf{g})]^+$ cation shows the usual syn–syn, anti–anti exchange at this temperature.

X-ray Structure of the Complex $[Pd(\eta^3\text{-}C_4H_7)(bpy)](CF_3SO_3)$. Although there was little doubt of the structure of $[Pd(\eta^3\text{-}C_4H_7)(\mathbf{a})]^+$ (R = H), it was important, both for the subtler aspects of the NMR NOE spectroscopy and for the modeling studies that follow, to increase our level of certainty with respect to the proton–proton separations pertinent to this discussion. An ORTEP view of the complex is shown in Figure 4. The molecule has a typical π-allyl palladium structure in that there is a distorted square-plane arrangement, assuming that the two terminal allyl carbons are taken as two of the four ligands. If we define a plane containing the Pd and the two nitrogen atoms, then the terminal carbons are 0.2 (C(7)) and 0.1 Å (C(9)) above the plane, whereas the central allyl carbon is 0.5 Å below. The allyl and Pt–N,N planes make an angle

(21) Faller, J. W.; Incorvia, M. J.; Thomsen, M. E. *J. Am. Chem. Soc.* **1969**, *91*, 518. Ammann, C.; Pregosin, P. S.; Rüegger, H.; Grassi, M.; Musco, A. *Magn. Reson. Chem.* **1989**, *27*, 355.

(22) Thorn, D. L.; Hoffmann, R. *J. Am. Chem. Soc.* **1978**, *100*, 2079. Tatsumi, K.; Hoffmann, R.; Yamamoto, A.; Stille, J. K. *Bull. Chem. Soc. Jpn.* **1981**, *54*, 1857.

(23) Li, M. P.; Drago, R. S.; Pribula, A. J. *J. Am. Chem. Soc.* **1977**, *99*, 6900.

(24) Addition of excess phenanthroline to $Pd(\eta^3\text{-}C_{10}H_{15})$(phenanthroline)$^+$ followed by a ^{1}H 2D exchange spectrum reveals that, although exchange takes place, an uncoordinated ligand is not involved.

(25) Faller, J. W. In *Advances in Organometallic Chemistry*; Academic Press: New York, 1977; p 211.

Table II. Selected Bond Lengths (Å), Bond Angles (deg), and Contact Distances (Å) for $[Pd(\eta^3\text{-}C_4H_7)(bpy)](CF_3SO_3)$

Pd–N(1)	2.089 (2)	$C(9)–H(9)_{anti}$	0.82 (3)
Pd–N(1′)	2.085 (3)		
		N(1′)–C(6′)	1.344 (4)
Pd–C(7)	2.095 (4)	N(1′)–C(2′)	1.346 (4)
Pd–C(8)	2.123 (4)	C(2′)–C(3′)	1.381 (4)
Pd–C(9)	2.112 (4)	C(3′)–C(4′)	1.389 (6)
		C(4′)–C(5′)	1.359 (6)
N(1)–C(6)	1.343 (4)	C(5′)–C(6′)	1.351 (6)
N(1)–C(2)	1.353 (4)		
C(2)–C(3)	1.376 (4)	$C(6')–H(9)_{syn}$	3.5
C(3)–C(4)	1.379 (5)	$C(6')–H(9)_{anti}$	3.7
C(4)–C(5)	1.362 (6)	$C(6)–H(7)_{syn}$	3.4
C(5)–C(6)	1.372 (5)	$C(6)–H(7)_{anti}$	3.9
C(2)–C(2′)	1.478 (4)	H(6′)–C(9)	3.1
C(6)–H(6)	0.83 (3)	$H(6')–H(9)_{anti}$	2.9
C(6′)–H(6′)	0.87 (4)	$H(6')–H(9)_{syn}$	3.1
		H(6)–C(7)	3.1
C(7)–C(8)	1.397 (6)	$H(6)–H(7)_{syn}$	2.8
C(8)–C(9)	1.380 (6)	$H(6)–H(7)_{anti}$	3.5
C(8)–C(10)	1.505 (6)		
		C(6′)–C(9)	3.62 (6)
$C(7)–H(7)_{syn}$	1.00 (4)	C(6)–C(7)	3.60 (6)
$C(7)–H(7)_{anti}$	1.02 (5)		
$C(9)–H(9)_{syn}$	1.11 (5)		

N(1)–Pd–N(1′)	78.67 (10)	C(4)–C(3)–C(2)	119.48 (34)
C(9)–Pd–C(7)	67.95 (22)	N(1)–C(2)–C(3)	120.62 (30)
C(9)–Pd–C(8)	38.03 (17)	C(2)–N(1)–C(6)	119.22 (30)
C(7)–Pd–C(8)	38.68 (16)	N(1)–C(6)–H(6)	120 (2)
		C(5)–C(6)–H(6)	118 (2)
N(1)–Pd–C(7)	106.42 (17)		
N(1′)–Pd–C(9)	106.71 (7)	N(1′)–C(6′)–C(5′)	122.72 (43)
		C(6′)–C(5′)–C(4′)	119.73 (38)
Pd–N(1′)–C(2′)	115.23 (19)	C(5′)–C(4′)–C(3′)	118.83 (36)
Pd–N(1′)–C(6′)	126.67 (27)	C(4′)–C(3′)–C(2′)	118.72 (36)
Pd–N(1)–C(2)	114.77 (19)	N(1′)–C(2′)–C(3′)	121.71 (29)
Pd–N(1)–C(6)	126.00 (25)	C(2′)–N(1′)–C(6′)	118.09 (32)
		N(1′)–C(6′)–H(6′)	112 (3)
Pd–C(9)–C(8)	71.40 (20)	C(5′)–C(6′)–H(6′)	125 (3)
Pd–C(7)–C(8)	71.72 (25)		
Pd–C(8)–C(7)	69.60 (23)	C(7)–C(8)–C(9)	115.72 (49)
Pd–C(8)–C(9)	70.57 (23)	C(7)–C(8)–C(10)	122.15 (48)
Pd–C(8)–C(10)	119.25 (28)	C(9)–C(8)–C(10)	121.16 (46)
N(1)–C(2)–C(2′)	115.71 (25)	$C(8)–C(7)–H(7)_{syn}$	116 (3)
C(3)–C(2)–C(2′)	123.65 (29)	$C(8)–C(7)–H(7)_{anti}$	119 (3)
N(1′)–C(2′)–C(2)	115.59 (25)	$C(8)–C(9)–H(9)_{syn}$	110 (2)
C(3′)–C(2′)–C(2)	122.70 (29)	$C(8)–C(9)–H(9)_{anti}$	120 (3)
N(1)–C(6)–C(5)	122.02 (41)		
C(6)–C(5)–C(4)	118.94 (36)	$H(9)_{syn}–C(9)–H(9)_{anti}$	128 (3)
C(5)–C(4)–C(3)	119.70 (33)	$H(7)_{syn}–C(7)–H(7)_{anti}$	116 (4)

of 109.4°, such that the C(central) to $-CH_3$ vector is pointed away from the metal. The two bite angles are 78.7 and 68.0° for the N–Pd–N and C(7)–Pd–C(9) angles, respectively, and the bond angles within bipyridyl are normal.[26] The Pd–N separations, 2.089 (2) and 2.085 (3) Å, as well as the Pd–C(allyl) distances, 2.095 (4), 2.123 (4), and 2.112 (4) Å, for C(7), C(8), and C(9), respectively, are not significantly different and are consistent with known literature values for related complexes.[27-29] We note that the Pd–C(allyl) separations are reasonable for an allyl trans to a ligand of moderate trans influence.[30] The $CF_3SO_3^-$ anion has been found, at a distance from the cation consistent with the usual van der Waals contacts. Bond separations and angles for the $[Pd(\eta^3\text{-}C_4H_7)(bpy)]^+$ cation are given in Table II.

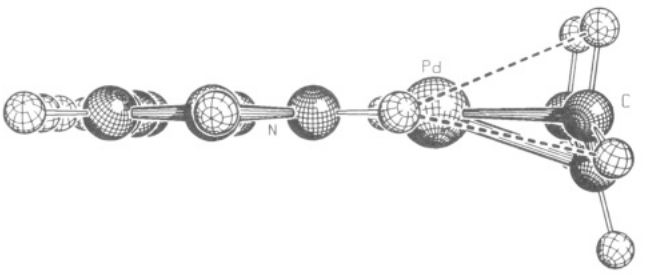

Figure 5. Side-on view of calculated structure for $Pd(\eta^3\text{-}C_3H_5)(bpy)^+$, showing distortion of anti protons out of the allyl plane.

Key hydrogen atoms on both of the ligands have been localized, and we point out once again[3] that since we expect distortions at allyl, this refinement is a worthwhile exercise. The pertinent distances (Å) from reporter protons on the bipyridyl to the allyl protons are H(6) to H(syn) = 2.8, H(6) to H(anti) = 3.5, H(6′) to H(syn) = 2.9, and H(6′) to H(anti) = 3.1.

There is a clear trend between the values for the syn and anti protons with respect to our "reporter" so that the observed NOE selectivity takes on additional meaning. Not surprisingly, the uncertainties are relatively large, so that only qualitative differences have significance. It is worth remembering that for bipyridine and phenanthroline we find strong selective interligand NOE's at separations of ca. 2.8 Å. Consequently, when biquinoline replaces bipyridine, the reporter allyl proton separation will drop to ca. 2.5 Å, and some loss of selectivity with respect to syn and anti NOE's is reasonable.

Molecular Modeling. In contrast to our palladium BINAP complex,[5] for which there was no structure available, for $Pd(\eta^3\text{-}C_4H_7)(bpy)^+$ we have the opportunity to combine NOE's, structure, and modeling. To this end, we have carried out semiempirical MO calculations and show the result in Figure 5, which demonstrates the relative position of CH_3, in accordance with theoretical expectations, as well as the distortion of the anti protons away from the metal. Assuming relatively long metal–ligand distances (ca. 2.2 Å for Pd–C(terminal) and ca. 2.14 Å for Pd–N) results in reporter proton–allyl proton separations of 2.9 and 3.4 Å for the syn and anti protons, respectively, in good agreement with the values found in the X-ray structure.

We take these calculations, combined with NOE's, to represent a satisfactory approach to measuring qualitative solution structures. Admittedly, our calculations are somewhat simplistic (see Experimental Section) and the NOE's are not quantitative; nevertheless, these shortcomings do not invalidate the approach, and we believe that more exact structures are likely in the future.

Experimental Section

^1H 2D NOESY spectra were obtained on WM-250, WH-300, and AM-600 Bruker spectrometers, using a standard three-pulse sequence.[31] The mixing time for the complexes of ligands **a**–**e** was chosen as 2.0 s, whereas for ligands **f** and **g** the value was 0.8 s (250 MHz). For **f** at 600 MHz, the value was 0.9 s. For complex **2**, the mixing time was 1.0 s. The decision for a given mixing time was based on T_1 measurements using an inversion–recovery se-

(26) Annibale, G.; Cattalini, L.; Bertolosi, V.; Ferretti, V.; Gestone, G.; Tobe, M. L. *J. Chem. Soc., Dalton Trans.* **1988**, 1265.
(27) Smith, A. E. *Acta Crystallogr.* **1965**, *18*, 331.
(28) Facchin, G.; Bertani, R.; Calligaris, M.; Nardin, G.; Mari, M. *J. Chem. Soc., Dalton Trans.* **1987**, 1381.
(29) Murrall, N. W.; Welch, A. J. *J. Organomet. Chem.* **1986**, *301*, 109.
(30) (a) Grassi, M.; Meille, S. V.; Musco, A.; Pontellini, R.; Sironi, A. *J. Chem. Soc., Dalton Trans.* **1989**, 615. (b) There are weak, but visible, cross peaks associated with the lowest and highest frequency CH_3 signals. They appear at different mixing times as well as at different B_0 field strengths. These could arise from exchange or from another source, e.g., spin diffusion. In any event they are sufficiently weak so as not to affect our conclusion. (c) We thank a reviewer for this suggestion.
(31) Derome, A. E. *Modern NMR Techniques for Chemistry Research*; Pergamon Press: Oxford, England, 1987; Vol. 6.

Table III. Microanalytical Data (%)

	calcd			found		
	C	H	N	C	H	N
1a, R = H	38.60	3.24	6.00	38.85	3.22	5.87
1a, R = CH_3	41.26	3.87	5.66	40.89	3.91	5.65
1b, R = H	41.60	3.08	5.71	41.31	3.17	5.75
1b, R = CH_3	43.98	3.69	5.40	43.57	3.82	5.43
1c	48.73	3.38	4.94	48.59	3.47	4.87
1d	33.74	4.14	6.05	33.15	4.11	5.74
1e	31.55	3.61	6.69	30.83	3.52	6.53
1f[a]	43.81	4.06	5.38	43.64	3.95	5.12
1f[b]	43.81	4.06	5.38	43.64	4.15	5.48
3	36.31	3.22	4.70	37.14	2.92	5.22

[a] Using *R*-PhCH(CH_3)NH_2 to form the imine. [b] Using *S*-PhCH(CH_3)NH_2 to form the imine.

Table IV. Experimental Data for the X-ray Diffraction Study of [Pd(η^3-C_4H_7)(bpy)](CF_3SO_3)

chem formula	$C_{15}H_{15}F_3N_2O_3PdS$
mol wt	466.76
crystal dimens, mm	0.25 × 0.30 × 0.35
data collcn *T*, °C	22
cryst syst	monoclinic
space group	$P2_1/c$
a, Å	7.185 (1)
b, Å	16.762 (1)
c, Å	14.811 (1)
β, deg	95.593 (9)
V, Å^3	1775.3
Z	4
ρ(calcd), g cm^{-3}	1.739
μ, cm^{-1}	11.88
radiation (λ, Å)	Mo Kᾱ graphite monochromated (0.710 69)
measd reflcns	$\pm h,+k,+l$
θ range, deg	$2.50 \le \theta \le 27.0$
scan type	$\theta/2\theta$
scan width, deg	1.10 + 0.35 tan θ
max counting time, s	65
bkgd time, s	0.5 (scan time)
max scan speed, deg min^{-1}	10.5
prescan rejection limit	0.55 (1.82 σ)
prescan acceptance limit	0.025 (40.00σ)
horiz receiving slit, mm	1.70 + tan θ
transm coeff	0.9665–0.9983
vert receiving slit, mm	4.0
no. of indep data	3854
no. of obs reflcns (n_o) ($\|F_o\|^2 > 2.0\sigma(\|F\|^2)$)	2676
no. of params refined (n_v)	286
R^a	0.031
R_w^b	0.043
GOF[c]	1.542

[a] $R = \sum\|\|F_o\| - 1/k\|F_c\|\|/\sum\|F_o\|$. [b] $R_w = [\sum w(\|F_o\| - 1/k\|F_c\|)^2/\sum w\|F_o\|^2]^{1/2}$, where $w = [\sigma^2(F_o)]^{-1}$ and $\sum F_o = [\sigma^2(F_o^2) + f^2(F_o^4)]^{1/2}/2F_o$, with $f = 0.045$. [c] GOF = $[\sum w(\|F_o\| - (1/k)\|F_c\|)^2/(n_o - n_v)]^{1/2}$.

quence. Ligands were purchased from Fluka AG. The π-allyl dimer [Pd(μ-Cl)(η^3-C_4H_7)]$_2$ was prepared according to the literature[32] in 84% yield. The cationic complexes were all prepared as follows.

[Pd(η^3-C_4H_7)(b)](CF_3SO_3). [Pd(μ-Cl)(η^3-C_4H_7)]$_2$ (42.3 mg, 1.07×10^{-4} mol) in 4 mL of methanol was treated with ligand **b** (41.8 mg, 2.26×10^{-4} mol) until a clear solution resulted. To the colorless solution that results was then added Tl(CF_3SO_3) (77 mg, 2.20×10^{-4} mol) with consequent immediate precipitation of a white solid. After being stirred stirring for 2 min, the suspension was filtered through Celite and the filtrate concentrated. The resulting solid was precipitated from $CHCl_3/Et_2O$, filtered out, and dried under vacuum to give 99.6 mg (94%) of product. Microanalytical data for the complexes are shown in Table III.

Table V. Final Positional Parameters and Equivalent Temperature Factors (Å^2) for [Pd(η^3-C_4H_7)(bpy)](CF_3SO_3)

atom	*x*	*y*	*z*	*B*[a]
Pd	0.17185 (4)	0.15198 (2)	0.08145 (2)	4.346 (5)
S	−0.3678 (2)	0.18652 (7)	0.36550 (8)	6.29 (3)
F(1)	−0.3373 (7)	0.0324 (2)	0.3660 (2)	14.3 (1)
F(2)	−0.4618 (7)	0.0774 (2)	0.4738 (2)	16.8 (1)
F(3)	−0.1805 (9)	0.0893 (3)	0.4692 (4)	20.0 (2)
O(1)	0.6454 (6)	0.2590 (2)	−0.0612 (3)	9.8 (1)
O(2)	0.7786 (6)	0.3056 (2)	−0.1880 (3)	10.6 (1)
O(3)	0.4541 (7)	0.3215 (4)	−0.1788 (4)	17.0 (2)
N(1)	0.1719 (4)	0.0491 (2)	0.1611 (2)	4.19 (6)
N(1′)	0.2380 (4)	0.0648 (2)	−0.0106 (2)	4.30 (6)
C(F)	−0.333 (1)	0.0923 (3)	0.4192 (3)	8.9 (2)
C(2)	0.2078 (4)	−0.0193 (2)	0.1175 (2)	4.07 (7)
C(2′)	0.2438 (4)	−0.0104 (2)	0.0215 (2)	4.02 (7)
C(3)	0.2135 (5)	−0.0912 (2)	0.1624 (3)	5.56 (9)
C(3′)	0.2839 (5)	−0.0743 (2)	−0.0322 (3)	5.56 (9)
C(4)	0.1849 (6)	−0.0931 (3)	0.2531 (3)	6.8 (1)
C(4′)	0.3171 (6)	−0.0601 (3)	−0.1215 (3)	6.8 (1)
C(5)	0.1466 (6)	−0.0243 (3)	0.2966 (3)	6.6 (1)
C(5′)	0.3105 (6)	0.0161 (3)	−0.1530 (3)	6.7 (1)
C(6)	0.1416 (6)	0.0462 (3)	0.2492 (3)	5.59 (9)
C(6′)	0.2719 (6)	0.0765 (3)	−0.0973 (3)	5.69 (9)
C(7)	0.0776 (7)	0.2450 (3)	0.1599 (4)	7.9 (1)
C(8)	0.1980 (6)	0.2771 (2)	0.1008 (3)	6.2 (1)
C(9)	0.1522 (7)	0.2611 (3)	0.0099 (3)	7.1 (1)
C(10)	0.3852 (8)	0.3115 (3)	0.1344 (4)	7.7 (1)
H(3)	0.238 (5)	−0.139 (2)	0.135 (2)	5.3 (9)*
H(3′)	0.286 (5)	−0.124 (2)	−0.008 (2)	4.9 (8)*
H(4)	0.197 (5)	−0.142 (2)	0.284 (2)	5.8 (9)*
H(4′)	0.338 (5)	−0.100 (2)	−0.160 (2)	5.8 (8)*
H(5)	0.120 (5)	−0.022 (2)	0.360 (2)	5.5 (8)*
H(5′)	0.336 (5)	0.028 (2)	−0.217 (2)	5.9 (8)*
H(6′)	0.264 (5)	0.126 (2)	−0.113 (3)	6.2 (9)*
H(6)	0.119 (4)	0.089 (2)	0.276 (2)	4.8 (8)*
H(71)	0.118 (6)	0.248 (3)	0.226 (3)	9 (1)*
H(72)	−0.065 (6)	0.248 (3)	0.142 (3)	9 (1)*
H(91)	0.271 (6)	0.278 (3)	−0.029 (3)	9 (1)*
H(92)	0.041 (5)	0.252 (2)	−0.010 (2)	5.3 (8)*
H(101)	0.400 (5)	0.316 (2)	0.198 (3)	6.8 (9)*
H(102)	0.482 (5)	0.281 (2)	0.116 (2)	6.6 (9)*
H(103)	0.405 (6)	0.360 (2)	0.110 (3)	7.0 (9)*

[a] Starred *B* values are for atoms that were refined isotropically. *B* values for anisotropically refined atoms are given in the form of the isotropic equivalent thermal parameter defined as $(4/3)[a^2B(1,1) + b^2B(2,2) + c^2B(3,3) + ab(\cos\gamma)B(1,2) + ac(\cos\beta)B(1,3) + bc(\cos\alpha)B(2.3)]$.

Yields of all the complexes were 60% and higher.

To obtain some feeling for the energetics of the exchange process, activation energies for the following were measured by using line shape analyses and standard equations for two-site exchange:[33]

	allyl	ligand	E_a, kJ/mol (±5%)
1	η^3-C_4H_7	**g**	72
2a	η^3-$C_{10}H_{15}$ (see 2)	**b**, R = CH_3	66
2b	η^3-$C_{10}H_5$ (1.5 equiv of H_2O added)	**b**, R = CH_3	68
3	$CH_2CH_2CH_2CH{-}C{-}CH_2$	**b**, R = CH_3	70

Crystallography. Crystals of [Pd(η^3-C_4H_7)(bpy)](CF_3SO_3) suitable for X-ray diffraction were obtained by crystallization from chloroform/tetrahydrofuran and are air stable.

A prismatic crystal was mounted on a glass fiber at a random orientation on an Enraf-Nonius CAD4 diffractometer for the unit cell and space group determination and for the data collection. Unit cell dimensions were obtained by least-squares fit of the 2θ values of 25 high-order reflections ($9.5 \lesssim \theta \lesssim 16.0$) by using the CAD4 centering routines. Selected crystallographic and other relevant data are listed in Table IV.

(32) Dent, W. D.; Long, R.; Wilkinson, A. J. *J. Chem. Soc.* **1964**, 1585. Powell, J.; Shaw, B. L. *J. Chem. Soc.* **1967**, 1839.

(33) Becker, E. D. *High Resolution NMR*; Academic Press: New York, 1980; p 243.

Data were measured with variable scan speed to ensure constant statistical precision on the collected intensities. Three standard reflections were used to check the stability of the crystal and of the experimental conditions and measured every 1 h; no significant variation was detected. The orientation of the crystal was checked by measuring three reflections every 300 measurements. Data have been corrected for Lorentz and polarization factors and for decay, using the data reduction programs of the CAD4 SDP package.[34] An empirical absorption correction was applied by using azimuthal (ψ) scans of three "high-χ-angle" reflections ($\chi \geq 86.6°$, $8.6° \leq \theta \leq 17.4°$). Transmission factors were in the range 0.9665–0.9983. The standard deviations on intensities were calculated in terms of statistics alone, while those on F_o were calculated as reported in Table IV. Intensities were considered as observed if $|F_o^2| > 2.0\sigma|F^2|$ and used for the solution and refinement of the structure. An $F_o = 0.0$ value was given to those reflections having negative net intensities.

The structure was solved by a combination of Patterson and Fourier methods and refined by full-matrix least squares[34] (the function minimized was $[\sum w(|F_o| - 1/k|F_c|)^2]$) with $w = [\sigma^2(F_o)]^{-1}$. No extinction correction was applied.

The scattering factors used, corrected for the real and imaginary parts of the anomalous dispersion, were taken from the literature.[34] Anisotropic temperature factors were used for all but the hydrogen atoms.

Most of the hydrogen atoms could be located in the final Fourier difference maps, in particular those of the allyl moiety and those bound to C(6) and C(6'), which were refined by using isotropic temperature displacements. The remaining hydrogens were also refined starting from their idealized positions (C–H = 0.95 Å, B = 5.0 Å^2).

Upon convergence (no parameter shift $\geq 0.4\sigma(p)$) the Fourier difference map showed no significant feature. All calculations were carried out by using the SDP crystallographic package.[35] Final atomic coordinates and thermal factors are given in Table V.

Modeling. The semiempirical MO package MOPAC V4.0[36] was used to generate molecular geometries on the AM1 level. The calculations used Zn instead of Pd as the metal center and were carried out for both C_3H_5 and C_4H_7 as the allyl ligand. The symmetry was defined as C_s. The separation between the metal atom and the center of the terminal C atoms of the π-allyl ligand was chosen as 1.85 Å, and a value of 109° was selected for the angle between the N–M–N and allyl planes. No other geometrical constraints were imposed. The total charge on the complex was assigned as +1 with the following found total charges: terminal allyl C, –0.52; central allyl C, +0.07; metal +0.703, nitrogen, –0.176.

Acknowledgment. We thank the ETH Zürich, the Swiss National Science Foundation, and the Italian CNR for support as well as the Johnson Matthey Research Centre, England, for the loan of palladium chloride. Special thanks are due to Drs. H. Rüegger and D. Moscau for measurements on the AM-600 spectrometer in Fällanden, Switzerland, as well as Michael Foxcroft and Roland Rapold for experimental assistance.

Supplementary Material Available: Tables of bond distances and bond angles (Table S1) and thermal parameters (Table S2) (4 pages); a listing of F_o and F_c values (Table S3) (27 pages). Ordering information is given on any current masthead page.

(34) *Enraf-Nonius Structure Determination Package, SDP*; Enraf-Nonius: Delft, The Netherlands, 1980.

(35) *International Tables for X-ray Crystallography*; Kynoch Press: Birmingham, England, 1974; Vol. IV.

(36) Stewart, J. J. P. MOPAC 4.0, QCPE Program 549. Quantum Chemistry Program Exchange, Indiana University.

Sterically Crowded Organometallics. Influence of Complexation upon the Conformation of Hexakis(phenylethyl)benzene

Michael J. Zaworotko*

Department of Chemistry, Saint Mary's University, Halifax, Nova Scotia, Canada B3H 3C3

K. Craig Sturge

Department of Chemistry, Dalhousie University, Halifax, Nova Scotia, Canada B3H 4J3

Luis Nunez and Robin D. Rogers*

Department of Chemistry, Northern Illinois University, DeKalb, Illinois 60115

Received October 2, 1990

In order to determine the relative importance of intraligand versus ligand–metal steric repulsions in sterically crowded arenes with flexible substituents, the effect of complexation upon the conformation of hexakis(phenylethyl)benzene (1) has been studied. X-ray crystallographic characterization of the free ligand and the hexafluorophosphate salt of its previously known complex with $[Fe(C_5H_5)]^+$, **2**, reveals that, whereas the ligand itself adopts the expected alternating three-up/three-down conformation, complexation forces an energetically unfavorable six-up (distal) conformation. To our knowledge, the latter represents the first example of such a conformation being exclusively adopted in the solid state. Furthermore, a VT-NMR study of **2** reveals no evidence of dynamic behavior, suggesting that the six-distal conformation also persists in solution. These results are discussed in the context of more widely studied hexaethylbenzene analogues. Crystal data: **1**, $C_{54}H_{54}$, triclinic, $P\bar{1}$, a = 11.567 (5) Å, b = 12.115 (6) Å, c = 15.887 (8) Å, α = 86.96 (5)°, β = 77.30 (5)°, γ = 76.01 (5)°, Z = 2, R = 0.070; **2**, $C_{59}H_{59}F_6FeP$, orthorhombic, $Pn2_1a$, a = 26.192 (9) Å, b = 18.447 (6) Å, c = 10.066 (7) Å, Z = 4, R = 0.074.

Introduction

Arene π-complexes are prototypal organometallic compounds and exist for virtually all the transition metals.[1] As such, they have engendered considerable attention, in particular because of the profound effect complexation has upon arene reactivity.[2] The depletion of π-electron den-

(1) Silverthorn, W. E. *Adv. Organomet. Chem.* **1975**, *13*, 47.

(2) Semmelhack, M. F.; Clark, G. R.; Garcia, J. L.; Harrison, J. J.; Thebtaranonth, Y.; Wulff, W.; Yamashita, A. *Tetrahedron* **1981**, *37*, 3957 and references therein.

0276-7333/91/2310-1806$02.50/0